Chemical Engineering Journal 157 (2010) 489–500

Contents lists available at ScienceDirect

Chemical Engineering Journal

journal homepage: www.elsevier.com/locate/cej

# Linear stability analysis of gas-fluidized beds for the prediction of incipient bubbling conditions

A. Busciglio, G. Micale*, G. Vella, L. Rizzuti

*Dipartimento di Ingegneria Chimica dei Processi e dei Materiali, Universitá degli Studi di Palermo, Viale delle Scienze, Ed. 6, 90128 Palermo, Italy*

ARTICLE INFO

*Article history:*
Received 20 July 2009
Received in revised form
23 November 2009
Accepted 21 December 2009

*Keywords:*
Gas fluidization
Stability criterion
Mathematical modelling

ABSTRACT

This work focuses on the development of a novel linear stability criterion for the state of homogeneous fluidization regime, based on a new mathematical model for gas-fluidized beds. The model is developed starting from the well-known particle bed model. A mono-dimensional momentum balance is derived leading to a set of equations which explicitly include voidage-gradient dependent terms (elastic force) for both solid and fluid phases.

A fully predictive criterion for the stability of homogeneous fluidization state is here proposed, based on the well-known Wallis' linear stability analysis. The criterion requires the choice of an appropriate averaging distance, which in the present development is found to be bed-voidage dependent. The linear stability criterion resulted in turn in a simple, yet fully predictive, relationship for incipient bubbling voidage.

Validation was carried out analyzing the influence of all physical properties and sensitivity to closure relations, showing substantial agreement with literature data.



## 1. Introduction and literature review

Fluidized beds are often attractive alternatives to fixed beds for several physical and chemical operation (*e.g.* heterogeneous catalytic reactions, drying, mixing, heating or cooling). The main advantages of fluidized beds are related to high heat and mass transfer coefficients, high degree of mixing within entire bed, due to the continuous circulation of solids. Thanks to these properties, fluidized beds are often smaller, more efficient and easy controlled than fixed beds.

The drawbacks are related to uncertainties in the design and scaling of equipment, due to the great complexity of fluidization hydrodynamics. For this reason the successful design of fluidized beds is strictly dependent on the development of advanced mathematical models. According to Ishii [22], fluidized beds are considered in the class of dispersed flows. Mathematical modelling of dispersed flows can be carried out adopting Eulerian–Lagrangian or Eulerian–Eulerian frameworks.

Eulerian–Eulerian models, also referred as two-fluid models (TFM), are actually the most frequently adopted for granular flow description. Both fluid and granular phase are treated in an almost symmetrical way, by using for each phase mass and momentum conservation equations typical of fluids.

General development of TFM, as presented in Enwald et al. [9], starts from integral conservation equation of mass, momentum and energy across phase boundaries. By applying Gauss and Leibniz theorems, local instantaneous conservation equations and relevant jump conditions are obtained. The subsequent step is the averaging procedure, suitably devised in order to avoid the condition of a space point in which only one phase exists, thus eliminating the consequent difficulty in momentum transfer calculation across phase boundary. An extensive literature was produced on averaging procedures [1,22,3,26,9]. Volume averaging is actually the most used in practical application, since it is possible to verify the scale separation condition.

Once averaging procedures are applied, the complete set of partial differential conservation equations is obtained (consisting of one volume fraction balance, two mass conservation equations and six momentum conservation equations to solve six velocity components, two volume fractions and pressure).

The most commonly used forms of conservation equations have been developed by Ishii [22] and Anderson and Jackson [1]. The Ishii model was originally developed for liquid–liquid flows and then was adapted to describe solid–fluid flows [8,9]. Conservation equations for both phases are exactly symmetrical, and momentum equations are both Navier–Stokes alike. Conversely, the Anderson and Jackson model was directly derived for gas–solid dispersed flows. It was originally formulated by Anderson and Jackson [1],

* Corresponding author. Tel.: +39 09123863780; fax: +39 0917025020.
*E-mail addresses:* a.busciglio@dicpm.unipa.it (A. Busciglio), micale@dicpm.unipa.it (G. Micale), vella@dicpm.unipa.it (G. Vella), rizzuti@dicpm.unipa.it (L. Rizzuti).

1385-8947/$ – see front matter © 2010 Elsevier B.V. All rights reserved.
doi:10.1016/j.cej.2009.12.040

**Nomenclature**

| | |
|---|---|
| $Ar$ | Archimedes number |
| $d_p$ | particles diameter [m] |
| $F$ | net force for unit volume [kg m$^{-2}$ s$^{-2}$] |
| $F_D$ | drag force for unit volume [kg m$^{-2}$ s$^{-2}$] |
| $g$ | gravitational acceleration [m s$^{-2}$] |
| $n$ | Richardson–Zaki expansion parameter |
| $P$ | pressure [Pa] |
| $u$ | local velocity [m s$^{-1}$] |
| $U_0$ | superficial gas velocity [m s$^{-1}$] |
| $u_D$ | dynamic wave velocity [m s$^{-1}$] |
| $u_k$ | kinematic wave velocity [m s$^{-1}$] |
| $u_t$ | terminal settling velocity [m s$^{-1}$] |

*Greek letters*

| | |
|---|---|
| $\alpha$ | particles phase volume fraction |
| $\delta$ | half of averaging length [m] |
| $\epsilon$ | fluid-phase volume fraction |
| $\mu$ | fluid viscosity [Pa s] |
| $\rho$ | density [kg m$^{-3}$] |
| $\Psi$ | generic scalar |

*Subscripts*

| | |
|---|---|
| $p$ | particles |
| $f$ | fluid |

and then revisited by Jackson alone [24–26]. The starting point is a set of local equations in the form of Navier–Stokes equations for the fluid phase and second Newton's law for particles. After averaging, a set of partial differential equations (PDE) is obtained, similar to Ishii's ones but with some remarkable differences between the fluid and solid phases equations.

Within the class of TFMs, Gibilaro and Foscolo developed the so-called particle bed model (PBM). The PBM is originated from Wallis' theory on the stability of homogeneous fluidization [48], where it is stated the need for a voidage-gradient dependent term in solid phase momentum balance to correctly predict the state of homogeneous expansion of fluidized beds. Wallis' theory, based on fluid bed characteristic wave velocities, was further developed by Foscolo and Gibilaro [11–14,17–19] who introduced the complete formulation and theoretical bases for the elastic behaviour of the fluidized beds. The PBM was eventually revisited by Gibilaro [16].

In this model the particle phase is considered as non-viscous and the isotropic contribution to the internal stress is considered negligible, thus eliminating the need for complete stress tensor formulation. Moreover, interparticle forces are also assumed negligible. Only fluid dynamic effects due to particle concentration gradients are considered through an elastic force contribution within the momentum balance of the solid phase. Different research groups have used the original PBM assumptions to develop new models for the description of fluidization hydrodynamics, such as Lettieri et al. [28], Brandani and Zhang [2]. PBM-based simulations have been compared with relevant experimental data [29,32,34], showing promising predictivity.

In particular, Brandani and Zhang [2] started from Foscolo and Gibilaro's PBM to derive a modified hydrodynamic model. They stated that the elastic term in the solid phase momentum balance equation, defined as an interphase force term (*i.e.* hydrodynamic interaction), does not disappear in overall momentum balance. Both phases are treated as continua without any statement about scale separation criteria or explicit averaging procedures. On this basis, Brandani and Zhang [2] derived a mathematical model in which the elastic force term is included in both fluid and solid phase momentum balance equations.

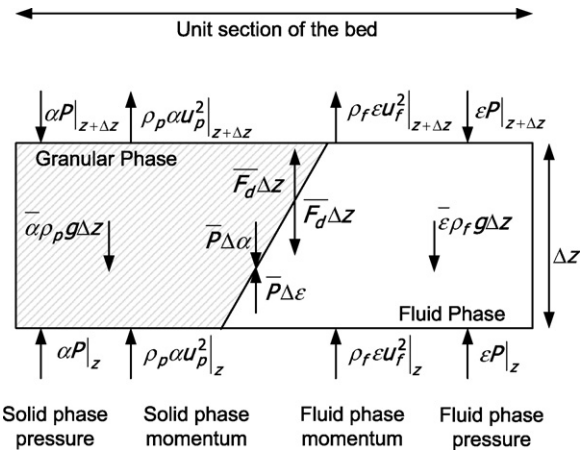


**Fig. 1.** Momentum balance scheme over a finite height section of a fluidized bed.

As far as mathematical closure of the conservation equations is concerned, it is necessary to completely specify momentum transfer between phases (drag forces). Drag forces for dense granular phases can be computed by suitably correcting the well-established correlations developed for isolated particle, or from pressure-drop correlation derived for packed beds [10,16,36,19,49,40,20,7,42,15,30,31].

On the above grounds, the present work stems from original PBM [16] and the modified formulation by Brandani and Zhang [2], with the aim to develop a new criterion for the prediction of the onset of bubbling fluidization. This will be accomplished through the development of a set of momentum equations including suitable elastic terms, and the coupling and the linearization of momentum equations.

## 2. Mathematical modelling

### 2.1. Hydrodynamic modelling

As mentioned earlier, the starting point for the derivation of the proposed stability criterion is the formulation of suitable momentum balance equations. The approach adopted in this work is that of Eulerian–Eulerian hydrodynamic modelling (two-fluid model), in which both granular and fluid phases are considered as interpenetrating fluids.

In particular, the derivation starts from taking into account only gravity, buoyancy and drag forces, with the solid phase defined non-viscous. A discrete momentum balance on both the fluid and the granular phase can be written in mono-dimensional fashion (*i.e.* along the vertical direction), with reference to a $\Delta z$ section of the bed, in which variation of volume fraction occurs, as sketched in Fig. 1:

$$\rho_p \frac{\partial \alpha u_p}{\partial t} = \rho_p[(\alpha u_p^2)_z - (\alpha u_p^2)_{z+\Delta z}] + [(\alpha P)_z - (\alpha P)_{z+\Delta z}] - \bar{\alpha}\rho_p g \Delta z + \bar{F}_D \Delta z + \bar{P}\Delta\alpha \quad (1)$$

$$\rho_f \frac{\partial \epsilon u_f}{\partial t} = \rho_f[(\epsilon u_f^2)_z - (\epsilon u_f^2)_{z+\Delta z}] + [(\epsilon P)_z - (\epsilon P)_{z+\Delta z}] - \bar{\epsilon}\rho_f g \Delta z - \bar{F}_D \Delta z + \bar{P}\Delta\epsilon \quad (2)$$

In this balance, time averaged properties are considered, and only spatial averaging procedure will be explicitly performed. The momentum balance for each phase, in classical Eulerian–Eulerian

formulation, considers symmetrical forces acting on the relevant control volume: momentum ($\rho_i u_i^2$), hydrostatic pressure ($P$), gravitational force ($\rho_i g$), interphase momentum exchange (drag force $F_D$) and hydrostatic pressure contribution at the interphase boundary. Each term is suitably multiplied by the relevant volume fraction. Notably, the forces acting on the interphase boundary are considered as acting on its center. Hydrostatic pressure field is the same for both phases. Properties which values have been considered at a suitable distance above the control volume bottom were indicated in general as $\bar{\Psi}$.

The momentum accumulation rate is intrinsically spatially averaged and therefore does not require any further average. Conversely, all terms in the form $\bar{\Psi}$ must be evaluated at $\Delta z/2$, since a linear variation of volume fraction is assumed to occur. As a consequence, the following equations can be written in a symmetrical form for both particle and fluid phases.

In the past, a number of works dealt with the modelling of interparticle forces [39,37,46,45,44] and tensional stresses due to particle attrition and flow [9]. In particular, it was shown [23,16] that the state of homogeneous fluidization, without the inclusion of suitable extra forces acting on the bed, is intrinsically unstable. Wallis [48] demonstrated that the inclusion of an elastic force acting on the granular phase can stabilize the state of homogeneous fluidization. Rietema and Piepers [39] reported that elastic forces can arise from the onset of a stable mechanical structure in homogeneously fluidized beds. Conversely, Gibilaro [16] and Brandani and Zhang [2] found that elastic forces arise from purely fluid dynamic interactions within the bed. In the present work the latter modelling approach is adopted and further developed. Of course, the need for inclusion of further terms explicitly accounting for interparticle forces will be discussed when presenting the results. With regard to tensional stresses, it must be reminded that the model to be proposed is aimed at the description of the incipient bubbling state, where granular phase motion is absent [37,43,33].

To accomplish the scale separation, the limit of Eqs. (1) and (2) for $\Delta z$ approaching to a finite value of $2\delta$ must be considered. In addition to limit computation, average properties included in Eqs. (1) and (2) have yet to be estimated. On the basis of the linear approximation considered, bed properties change linearly along $z$ direction. Therefore, for a generic scalar quantity evaluated at the height $z+\delta$ the following equality can be written:

$$\bar{\Psi} = \Psi + \delta \frac{\Delta \Psi}{\Delta z} \tag{3}$$

The above expression may be adopted for each scalar quantity not yet averaged in Eqs. (1) and (2); dividing by $\Delta z$, the following expression is obtained for solid phase:

$$\rho_p \frac{\partial \alpha u_p}{\partial t} = \rho_p \frac{-\Delta\left(\alpha u_p^2\right)}{\Delta z} + \frac{-\Delta\left(\alpha P\right)}{\Delta z} - \left[\alpha + \delta \frac{\Delta \alpha}{\Delta z}\right] \rho_p g + \left[F_D + \delta \frac{\Delta F_D}{\Delta z}\right] + \left[P + \delta \frac{\Delta P}{\Delta z}\right] \frac{\Delta \alpha}{\Delta z} \tag{4}$$

Similar equation is obtained for fluid-phase momentum balance equation.

The ratios can be now substituted with the relevant partial derivatives, being equal to first order terms inside the control volume considered:

$$\rho_p \frac{\partial \alpha u_p}{\partial t} = -\rho_p \frac{\partial(\alpha u_p^2)}{\partial z} + \left[F_D + \delta \frac{\partial F_D}{\partial z}\right] - \left[\alpha + \delta \frac{\partial \alpha}{\partial z}\right] \rho_p g - \frac{\partial(\alpha P)}{\partial z} + P \frac{\partial \alpha}{\partial z} + \delta \frac{\partial P}{\partial z} \frac{\partial \alpha}{\partial z} \tag{5}$$

The differential form of the momentum balance equation is finally obtained by neglecting the second order terms, such as that including the product of the pressure gradient and the volume fraction gradient. By applying the same procedure to the fluid-phase discretized momentum balance, the full set of momentum conservation equations can be derived. Drag force derivatives with respect to $z$ coordinate are reported as in the following:

$$\frac{\partial F_D}{\partial z} = \frac{\partial F_D}{\partial \epsilon} \frac{\partial \epsilon}{\partial z} = \frac{\partial F_D}{\partial \alpha} \frac{\partial \alpha}{\partial z} \tag{6}$$

The final momentum balance equations (Eqs. (8) and (7)), relevant continuity equations (Eqs. (9) and (10)) and the volume fraction balance equation (Eq. (11)) are reported in the following:

$$\rho_p \left( \frac{\partial \alpha u_p}{\partial t} + \frac{\partial(\alpha u_p^2)}{\partial z} \right) = F_D - \alpha \left[\rho_p g + \frac{\partial P}{\partial z}\right] + \delta \left[\frac{\partial F_D}{\partial \alpha} - \rho_p g\right] \frac{\partial \alpha}{\partial z} \tag{7}$$

$$\rho_f \left( \frac{\partial \epsilon u_f}{\partial t} + \frac{\partial(\epsilon u_f^2)}{\partial z} \right) = -F_D - \epsilon \left[\rho_f g + \frac{\partial P}{\partial z}\right] - \delta \left[\frac{\partial F_D}{\partial \epsilon} + \rho_f g\right] \frac{\partial \epsilon}{\partial z} \tag{8}$$

$$\frac{\partial \epsilon}{\partial t} + \frac{\partial \epsilon u_f}{\partial z} = 0 \tag{9}$$

$$\frac{\partial \alpha}{\partial t} + \frac{\partial \alpha u_p}{\partial z} = 0 \tag{10}$$

$$\epsilon + \alpha = 1 \tag{11}$$

With reference to right-hand side (R.H.S.) of momentum equation, it is worth noting that, in addition to drag, gravity and buoyancy, an extra term appears. Notably, the use of a finite length for spatial averaging, large enough to include in the control volume a piecewise linear variation in the volume fraction along the $2\delta$ vertical distance, leads to the appearance of a term in momentum balance equations which is dependent on the $\delta$ parameter and the voidage gradient. Such term is quite similar in its expression to the extra momentum term developed by Foscolo and Gibilaro [12] in the original PBM, accounting for the elastic behaviour of the granular phase. Moreover, it was demonstrated [48] that the coefficient of the voidage-gradient dependent term is proportional to the square of the shock propagation velocity $u_D$ in the relevant phase.

The symmetrical derivation of momentum balance equations leads to the presence of an elastic term in both solid- and fluid-phase equations. These elastic extra terms are obviously dependent on the formulation of averaging length $\delta$ and drag force. The theoretical derivation of a closed formula for estimating $\delta$ will be discussed in the next sections.

### 2.2. Constitutive equations and equilibrium conditions

The trivial steady state solution of the fluidized bed equations implies an uniform expansion of the bed under given conditions of inlet gas velocity and particle properties. The homogeneously fluidization state is stable if any small voidage perturbation starting in a point of the bed will decrease its intensity along its path. Otherwise, homogeneous fluidization is an unstable condition, *i.e.* any voidage perturbation will became larger along its path through the bed. On this basis, the homogeneous fluidization state will be subsequently regarded as the equilibrium condition, for any given particle system and fluid velocity.

One of the fundamental relations for the description of homogeneously fluidized bed is the well know Richardson–Zaki expansion law [36], linking inlet gas superficial velocity $U_0$ with particle and fluid bed characteristics (voidage $\epsilon$ and particle settling velocity

$u_t$):

$$U_0 = u_t \epsilon^n \tag{12}$$

where the exponent $n$ was theoretically found to be bounded by the values 2.4 for inertial regime and 4.8 for viscous regime.

In this work a drag force formulation based on the Richardson–Zaki expansion law [36] is adopted, as derived by Gibilaro [16]:

$$F_D = \frac{1-\epsilon}{\epsilon^{3.8}}(\rho_p - \rho_f) g \left( \frac{U_0 - u_p}{u_t} \right)^{4.8/n} \tag{13}$$

Explicit expressions for drag force and its derivative will be needed for the formulation of the stability criteria. Near-equilibrium approximations can be used to formulate simpler linear stability analysis. The use of an equilibrium formulation can correctly consider the instability phenomena arising from small perturbations of an initial equilibrium condition, nevertheless giving much simpler formulations.

The equilibrium conditions for the homogeneously fluidized bed can be written as follows:

$$\begin{cases} u_p = 0 \\ U_0 = u_t \epsilon^n \end{cases} \tag{14}$$

where the second equality is the Richardson–Zaki expansion law. By substituting Eq. (14) into Eq. (13), the following expressions for near-equilibrium drag force and relevant partial derivative with respect to voidage are obtained:

$$F_{D,ne} = \epsilon(1-\epsilon)(\rho_p - \rho_f) g \tag{15}$$

$$\frac{\partial F_{D,ne}}{\partial \epsilon} = (1-2\epsilon)(\rho_p - \rho_f) g \tag{16}$$

Two other drag force expressions will be considered for the purpose of comparison, both reported by Gibilaro [16]:

$$F_D = \frac{3\rho_f U^2}{4 d_p} \left( 0.63 + \frac{4.8}{Re_p^{0.5}} \right)^2 (1-\epsilon)\epsilon^{-3.8} \tag{17}$$

$$F_D = \frac{\rho_f U^2}{d_p} \left( 0.33 + \frac{18}{Re_p} \right) (1-\epsilon)\epsilon^{-3.8} \tag{18}$$

The first relation (Eq. (17)) is the expression for single particle drag force [5], corrected for dense bed condition [49], hereafter referred as DV drag. The second relation is a modified Ergun equation developed by Gibilaro et al. [19], hereafter referred as ME drag (Eq. (18)).

The expression for near-equilibrium drag forces in both cases are obtained by inserting Eq. (14), respectively, into Eqs. (17) and (18):

$$F_{D,ne} = \frac{3\rho_f u_t^2}{4 d_p} \left( 0.63 + \frac{4.8}{Re_t^{0.5} \epsilon^{0.5n}} \right)^2 \frac{(1-\epsilon)}{\epsilon^{3.8-2n}} \tag{19}$$

$$F_{D,ne} = \frac{\rho_f u_t^2}{d_p} \left( 0.33 + \frac{18}{Re_t \epsilon^n} \right) \frac{(1-\epsilon)}{\epsilon^{3.8-2n}} \tag{20}$$

### 2.3. Momentum equation coupling

General two-phase coupling [16] is achieved getting the pressure gradient from the fluid-phase momentum equation (Eq. (8)), and then substituting it in the particle phase momentum equation (Eq. (7)).

The general form of pressure gradient can be obtained from the fluid-phase momentum equation:

$$\frac{\partial P}{\partial z} = -\rho_f \left( \frac{\partial \epsilon u_f}{\partial t} + \frac{\partial (\epsilon u_f^2)}{\partial z} \right) - \frac{F_D}{\epsilon} - \rho_f g + \frac{1}{\epsilon} \left( -\frac{\partial F_D}{\partial \epsilon} - \rho_f g \right) \delta \frac{\partial \epsilon}{\partial z} \tag{21}$$

This general procedure can be particularized for gas fluidization, by introducing the negligible gas-density hypothesis, *i.e.* any gas-density dependent term of the fluid momentum equation is considered negligible with respect to solid-density dependent terms. This assumption is valid in the case of gas fluidization, in which gas-density is about three orders of magnitude smaller than solid density. The pressure gradient previously derived for general phase coupling (Eq. (21)) can be now written as in the following:

$$\left. \frac{\partial P}{\partial z} \right|_{\rho_f = 0} = -\frac{1}{\epsilon} \left( F_D + \delta \frac{\partial F_D}{\partial \epsilon} \frac{\partial \epsilon}{\partial z} \right) \tag{22}$$

In this approach inertial terms depending on gas-density are neglected. Conversely, the elastic force and the drag force affect the pressure gradient profile, and therefore the global hydrodynamics. Such a mathematical development where the fluid-phase elastic term is present will be hereafter referred as partial decoupling approach (PDA). This is quite different from what could be obtained applying the same procedure to the original PBM momentum equations [16], since the elastic term does not appear in the fluid-phase momentum balance equation.

Eqs. (15) and (16) for near-equilibrium drag force can be easily substituted into Eq. (22) to obtain a simple formulation of pressure gradient:

$$\left. \frac{\partial P}{\partial z} \right|_{PDA} = (1-\epsilon)(\rho_p - \rho_f) g + \frac{(1-2\epsilon)(\rho_p - \rho_f) g}{\epsilon} \delta \frac{\partial \epsilon}{\partial z}. \tag{23}$$

Starting from the PDA, a further simplification can be made by substituting Eqs. (15) and (16) into Eq. (22) and neglecting the elastic term:

$$\left. \frac{\partial P}{\partial z} \right|_{TDA} = (1-\epsilon)(\rho_p - \rho_f) g \tag{24}$$

The resulting equations (Eq. (24)) will be hereafter referred as total decoupling approach (TDA). Notably, the TDA will lead to the same results of the original PBM, if a suitable constant value of the $\delta$ length is adopted.

In order to derive a coupled equation to describe the behaviour of small voidage perturbations travelling along the fluidized bed Eqs. (13) and (11) are inserted in the R.H.S. of the solid phase momentum balance equation (Eq. (7)):

$$\rho_p \left( \frac{\partial \alpha u_p}{\partial t} + \frac{\partial (\alpha u_p^2)}{\partial z} \right) = (1-\epsilon) \left[ \frac{(\rho_p - \rho_f) g}{\epsilon^{3.8}} \left( \frac{U_0 - u_p}{u_t} \right)^{4.8/n} \right] - (1-\epsilon) \left[ \rho_p g + \frac{\partial P}{\partial z} \right] + \delta \left( \frac{\partial F_D}{\partial \epsilon} + \rho_p g \right) \frac{\partial \epsilon}{\partial z} \tag{25}$$

By rearranging and putting in evidence the voidage-gradient dependent terms, the following coupled balance equation is obtained:

$$\rho_p \left( \frac{\partial \alpha u_p}{\partial t} + \frac{\partial (\alpha u_p^2)}{\partial z} \right) = F + \delta \left( \frac{\partial F_D}{\partial \epsilon} + \rho_p g \right) \frac{\partial \epsilon}{\partial z} \tag{26}$$

The net force term $F$ includes, in its complete non-equilibrium expression, drag, pressure gradient and gravity terms:

$$F_{\text{net}} = (1-\epsilon) \left[ \frac{(\rho_p - \rho_f) g}{\epsilon^{3.8}} \left( \frac{U_0 - u_p}{u_t} \right)^{4.8/n} \right] - (1-\epsilon) \left[ \rho_p g + \frac{\partial P}{\partial z} \right] \tag{27}$$

For PDA the final coupled momentum equation is obtained by substituting the relevant expression of the pressure gradient (Eq. (23)) in Eq. (27), and the relevant partial derivative of drag force (Eq. (16))

in Eq. (26). By rearranging, the following is obtained:

$$\rho_p \left( \frac{\partial \alpha u_p}{\partial t} + \frac{\partial \alpha u_p^2}{\partial z} \right) = F_{\mathrm{PDA}} + \rho_p u_B^2 \frac{\partial \epsilon}{\partial z} \tag{28}$$

$$F_{\mathrm{PDA}} = (1-\epsilon)(\rho_p - \rho_f) g \left[ \frac{1}{\epsilon^{3.8}} \left( \frac{U_0 - u_p}{u_t} \right)^{4.8/n} - \epsilon \right] \tag{29}$$

$$u_{D,\mathrm{PDA}}^2 = \frac{(1-\epsilon)}{\epsilon} \delta g \tag{30}$$

where the dynamic velocity $u_{D,\mathrm{PDA}}$ appears.

The same procedure can be adopted by using the TDA equations for near-equilibrium pressure gradient, *i.e.* Eq. (24) instead of Eq. (23). Eventually, equations identical to Eqs. (28) and (29) are obtained, with the only difference in the formulation of the dynamic velocity (Eq. (30)), as reported below:

$$u_{D,\mathrm{TDA}}^2 = 2(1-\epsilon)\delta g \tag{31}$$

## 3. Linear stability criteria

As discussed in detail elsewhere [16], the linear stability analysis is based on the decomposition of variables of the coupled momentum equation (Eq. (28)). In particular, voidage is expressed as the sum of two terms: an equilibrium value $\epsilon_0$ plus a deviation from equilibrium $\epsilon^*$; particle velocity equilibrium value is assumed to be zero, so that particle velocity deviation value coincides with $u_p$. Under the hypothesis of near-equilibrium conditions, the relevant Taylor expansion of Eq. (28) leads to a travelling wave equation for the $\epsilon^*$ variable. The solution of this linearized equation reveals that all voidage perturbation wave velocities in the bed are bounded by the kinematic wave velocity (long wave) and the dynamic wave velocity (short wave).

In general, the condition for the exponential decline of a voidage perturbation amplitude along the bed (necessary for stable behaviour of homogeneous fluidization) is that $u_D$ is higher than the kinematic wave velocity $u_k$. In form of dimensionless stability function $S$:

$$S = \frac{u_D - u_k}{u_k} \begin{cases} > 0 & \text{homogeneous} \\ = 0 & \text{incipient bubbling} \\ < 0 & \text{bubbling} \end{cases} \tag{32}$$

In this work, the kinematic wave velocity expression developed by Gibilaro [16] is adopted:

$$u_k = n u_t (1-\epsilon)\epsilon^{n-1} \tag{33}$$

### 3.1. Definition of the length parameter

Both Eqs. (30) and (31) needs the definition of the $\delta$ length, and therefore the height of the finite control volume. For this purpose, in mono-dimensional formulation, a control volume can be taken in which a perturbation of the flow field starts at the bottom. This perturbation needs a time interval $\Delta t$ to travel through the first particle layer of height $d_p$, and this time interval depends on the average interstitial gas velocity. It is computed according to the equilibrium expansion law proposed by Richardson and Zaki [36]:

$$\Delta t = \frac{d_p}{u_f} = \frac{d_p}{U_0/\epsilon} = \frac{d_p}{u_t \epsilon^{n-1}} \tag{34}$$

During the same time interval $\Delta t$, a voidage perturbation travels through the control volume at the kinematic wave velocity, by assuming that the wave passage leads to an instantaneous change of voidage from the initial equilibrium value to the final. The kinematic wave velocity actually travels along a distance $\delta$ equal to half height of the control volume in the time interval $\Delta t$, as reported in the following expression:

$$\Delta t = \frac{\delta}{n u_t (1-\epsilon)\epsilon^{n-1}} \tag{35}$$

Under these hypotheses, the full range of states involved in voidage perturbation initiation would occur within the whole control volume:

- the flow perturbation is located at the bottom of the control volume;
- the idealized kinematic wave is located at half height;
- the top is surely not affected by any perturbation, even if the front of the kinematic wave is dispersed by inertial effects.

Such definition of the control volume is certainly valid for a linear stability analysis, where the incipient bubbling state implies the equality of characteristic wave velocities, thus avoiding any perturbation to travel faster than the kinematic waves.

Eventually, by comparing Eqs. (34) and (35) the time interval $\Delta t$ disappears:

$$\delta = (1-\epsilon) n d_p \tag{36}$$

In mono-dimensional formulation, these assumptions lead to the definition of a control volume height variable with voidage. This is a substantial new result in fluidized bed modelling, with respect to both PBM [16] and the Brandani and Zhang model [2], that will be hereafter referred in the following as BZM. Remarkably it was obtained without any particular assumption but the validity of the Richardson and Zaki [36] expansion law.

Once the averaging length is defined, Eq. (36) can be substituted in Eqs. (30) and (31) to obtain the final expressions for $u_B$ in the case of TDA and PDA, respectively. Remarkably, the main difference of the present formulation with respect to those by Gibilaro [16] and Brandani and Zhang [2] lies in the expression of the dynamic velocity $u_D$ in terms of functional dependence from the local voidage:

$$\begin{cases} u_{D,\mathrm{TDA}}^2 = 2 n d_p g (1-\epsilon)^2 \\ u_{D,\mathrm{PDA}}^2 = n d_p g (1-\epsilon)^2 \epsilon^{-1} \\ u_{D,\mathrm{PBM}}^2 = 3.2 d_p g (1-\epsilon) \\ u_{D,\mathrm{BZM}}^2 = d_p g (1-\epsilon)\epsilon^{-1} \end{cases} \tag{37}$$

Substituting these expressions in the stability function reported in Eq. (32), two fully predictive stability criteria can be obtained, *i.e.* the total decoupling (TDA) and the partial decoupling (PDA) criterion:

$$\begin{cases} \mathrm{TDA} \rightarrow \epsilon_{mb} = \left( \dfrac{2 g d_p}{n u_t^2} \right)^{\dfrac{0.5}{n-1}} \\ \mathrm{PDA} \rightarrow \epsilon_{mb} = \left( \dfrac{g d_p}{n u_t^2} \right)^{0.5/(n-0.5)} \end{cases} \tag{38}$$

Formulation of both criteria does not include adjustable parameters, therefore leading to fully predictivity. The TDA-based criterion neglects the influence of the elastic term in the fluid-phase momentum balance, thus resulting analogue to the stability criterion obtained on the basis of the PBM, with the exception derived by the use of a voidage dependent term in averaging length. This fact lead to a notably different behaviour of the stability function, as will be extensively discussed in the next sections of this work. Conversely, the PDA-based criterion includes both new assumption of the model, *i.e.* the elasticity of the fluid phase, as in Brandani and

Zhang [2], and the use of a voidage dependent averaging length. However, in the BZM a constant averaging length equal to $d_p$ is adopted in order to best fit literature data on minimum bubbling voidage. In the present formulation, the averaging length is theoretically derived and found to be dependent on local voidage.

## 4. Results and discussion

The two previously derived approaches will be now analyzed, *i.e.* the total decoupling approach (TDA) and the partial decoupling approach (PDA). The latter is the most general criterion for the case of gas fluidization, while the former is derived under the further hypothesis of negligibility of the elasticity term in the fluid phase. Both criteria are fully predictive, and they just need a closure relationship to estimate the Richardson and Zaki [36] parameter $n$ and the terminal settling velocity of particles, $u_t$. For the sake of comparison, the correlations used in this work for such estimates are the same used by Gibilaro [16]:

$$Ar = \frac{g d_p^3 \rho_f (\rho_p - \rho_f)}{\mu_f^2} \tag{39}$$

$$n = \frac{4.8 + 0.1042 Ar^{0.57}}{1 + 0.043 Ar^{0.57}} \tag{40}$$

$$u_t = \frac{\mu_f}{\rho_f d_p}\left[\left(-3.809 + 3.809^2 + 1.832 Ar^{0.5}\right)^{0.5}\right]^2 \tag{41}$$

The original PBM formulation leads to the following stability criterion to predict incipient bubbling voidage:

$$\frac{1.79}{n}\left(\frac{g d_p}{u_t^2}\right)^{0.5}\left(\frac{\epsilon_{mb}^{1-n}}{(1-\epsilon_{mb})^{0.5}}\right) = 1 \tag{42}$$

The stability criterion of the BZM is obtained by the substitution of $\delta$ with $d_p$ as averaging length in the PDA formulation of the dynamic wave velocity. This leads to a quite similar dependency on voidage with respect to the original PBM stability criterion:

$$\frac{1}{n}\left(\frac{g d_p}{u_t^2}\right)^{0.5}\left(\frac{\epsilon_{mb}^{0.5-n}}{(1-\epsilon_{mb})^{0.5}}\right) = 1 \tag{43}$$

The influence of several physical parameters such as gas phase pressure (influencing mainly gas-density and viscosity), temperature, particle diameter and density, strength of gravitational field will be compared with literature data. Table 1 summarizes the parameters and their relevant ranges here analyzed.

**Table 1**
Parameters tested.

| Parameter | Range |
|---|---|
| Temperature [°C] | 25–900 |
| Pressure [bar] | 1–140 |
| $g_s/g$ | 1–3 |
| Particle density [kg/m$^3$] | 500–2500 |
| Particle diameter [μm] | 20–140 |

The prediction of both PDA and TDA criteria have been validated with literature data. Moreover the predictions by the original particle bed model and the model proposed by Brandani and Zhang [2] will be also reported for the sake of a complete critical analysis. MBV predictions by means of PDA using different equations for the drag force (Eqs. (19) and (20)) will be reported only in a later section. Relevant stability criteria analytical expressions are not reported here.

### 4.1. Temperature effect

The effect of temperature is reported in Fig. 2. In particular, in Fig. 2(a) experimental results obtained by Rowe [41] are shown in terms of minimum bubbling voidage (MBV) of fine FCC catalyst at temperatures between 25 and 500 °C. Experimental data show an increase of MBV mainly due to the increased viscosity of the gas phase. Prediction of TDA and PDA are both correct in estimating data trends, although an overestimate is evident. BZM also shows

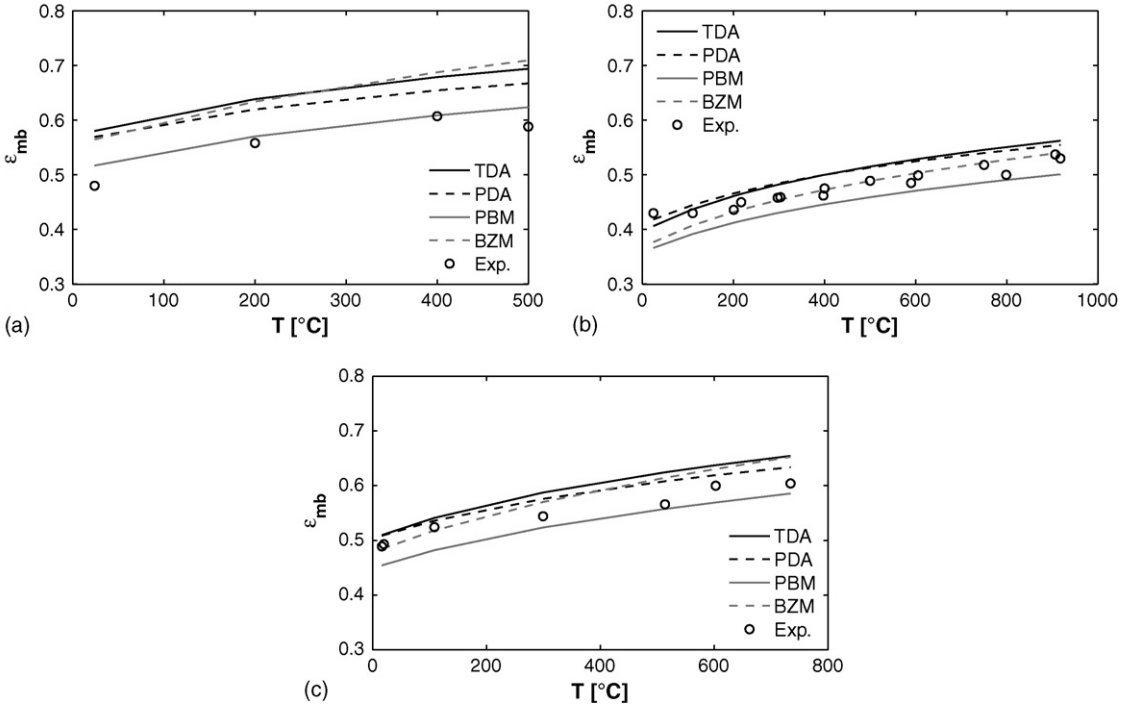


**Fig. 2.** Temperature effect on MBV [41,35]: (a) MBV of FCC catalyst (75 μm) fluidized by air; (b) MBV of FCC catalyst (103 μm) fluidized by nitrogen; (c) MBV of FCC catalyst (65 μm) fluidized by nitrogen.

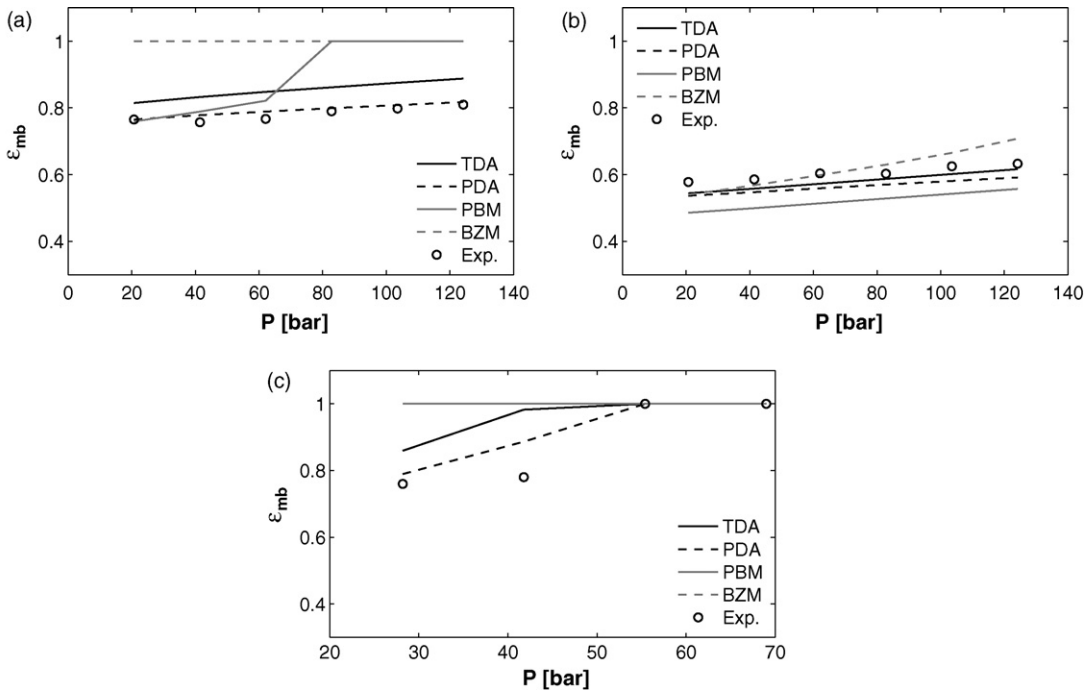


**Fig. 3.** Pressure effect on MBV [27,4]: (a) MBV of carbon powder (44 μm) fluidized by syngas; (b) MBV of carbon powder (112 μm) fluidized by syngas; (c) MBV of carbon powder (63 μm) fluidized by $CF_4$.

an overestimate which furthermore increases with temperature. Average overestimate by TDA and BZM is about 16%, while PDA shows an average discrepancy of 13%. For this data set, the PBM predictions are the best.

In Fig. 2(b) and (c) the experimental results by Rapagná et al. [35] are shown for the case of a FCC catalyst at temperatures between 25 and 900 °C. The predictions are correct for all models with PBM showing an optimal match for temperatures up to 200 °C. TDA and PDA slightly overestimate MBV values (5%), while PBM predictions show a slight underestimation of MBV.

Other literature data on the effect of operating temperature have been considered [28,32,21]; they will be reported in a later section on overall model predictivity.

### 4.2. Pressure effect

The pressure effect on MBV is shown in Fig. 3. Pressure mainly influences the gas-density value, resulting in an increase of MBV with pressure. Pressure and temperature are taken in ranges for which gas viscosity variations are negligible or second order effects. In Fig. 3(a) and (b) experimental data by Jacob and Weimer [27] are shown (particles with $d_p = 44\,\mu m$ in the former, $d_p = 112\,\mu m$ in the latter, fluidized with syngas $H_2/CO_{vol} = 0.8$, $P = 20$–$120$ bar). In Fig. 3(a) it is possible to observe that the prediction of MBV by TDA are in very good agreement with experimental data, while PDA shows an average overestimate (less than 10%) of MBV values. BZM failed to predict the transition between particulate to bubbling fluidization, because of the sensitivity of the stability function at high voidage bubbling systems. The PBM appears to be less sensitive to the numerical stability of the criterion with respect to BZM stability function, but for high MBV values this model also appears to uncorrectly predict the fluidization regime transition.

Fig. 3(b) shows that the predictions of MBV values by PDA and TDA slightly underestimate (less than 7% for PDA, less than 4% for TDA) MBV values. BZM underestimates MBV at low pressures and overestimates MBV at high pressures, PBM systematically underestimates MBV of about 15%.

In Fig. 3(c) the experimental results by Crowther and Whitehead [4] are shown (carbon powder, 63 μm fluidized with $CF_4$) with pressures ranging from 30 to 70 bar. The systems reported exhibit high MBV at lower pressures and absence of bubbling at higher pressures. It can be clearly observed that the TDA better predicts the behaviour of the powder at all pressures. The PDA shows similar predictions but with higher overestimates at lower pressures, while both the PBM and the BZM fail to predict the transition from homogeneous to bubbling fluidization.

Other literature data on the effect of operating pressure have been tested [47] but they will be reported in a later section on overall model predictivity.

### 4.3. Gravitational field strength effect

In Figs. 4 and 5 the data by Rietema and Mutsers [38] on the effect of gravitational field strength are analyzed. The authors adopted different granular materials (FCC catalyst and polypropylene particles, PP) with different gases ($H_2$, $N_2$) in a centrifuge in which the gravitational field strength was varied from the normal value to three times the normal value. The experimental results show a decreasing trend in MBV, mainly due to an increased weight of particles, somewhat similar to an increase in particle density.

Fig. 4(a), in which PP/$H_2$ data are reported, shows an underestimation (between 18% and 27%) of MBV values for all models, with TDA showing the minimum underestimation and the PBM the maximum underestimation. Predictions for the system PP/$N_2$, reported in Fig. 4(b), show that both PDA and TDA correctly predict MBV values with slight underestimates (less than 4% for TDA, less than 7% for PDA), while BZM behaves differently, especially near standard gravity. Conversely PBM predictions results in the largest underestimations of the MBV. In Fig. 5(a) the system FCC/$H_2$ is shown, for which all models give correct predictions, with slight underestimates in MBV values, larger for PBM and BZM (about 20%), and smaller for TDA and PDA (14%). In Fig. 5(b) data for FCC/$N_2$ system are shown, for which prediction of MBV by PDA and TDA are substantially overlapped and in excellent agreement with experimental data, while PBM and BZM predictions suffer from a

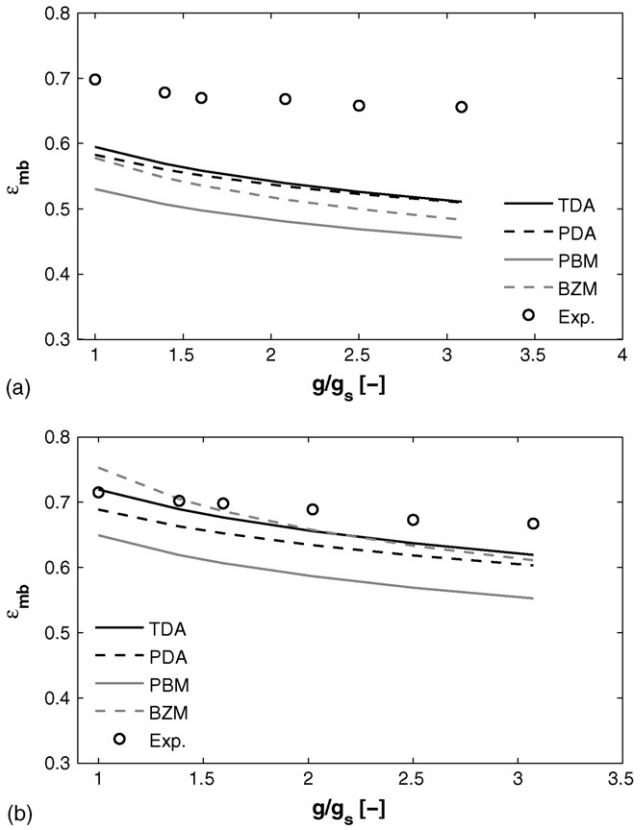


**Fig. 4.** Gravitational field strength effect on MBV of polypropylene particles [38]: (a) incremented gravity (hydrogen) and (b) incremented gravity (nitrogen).

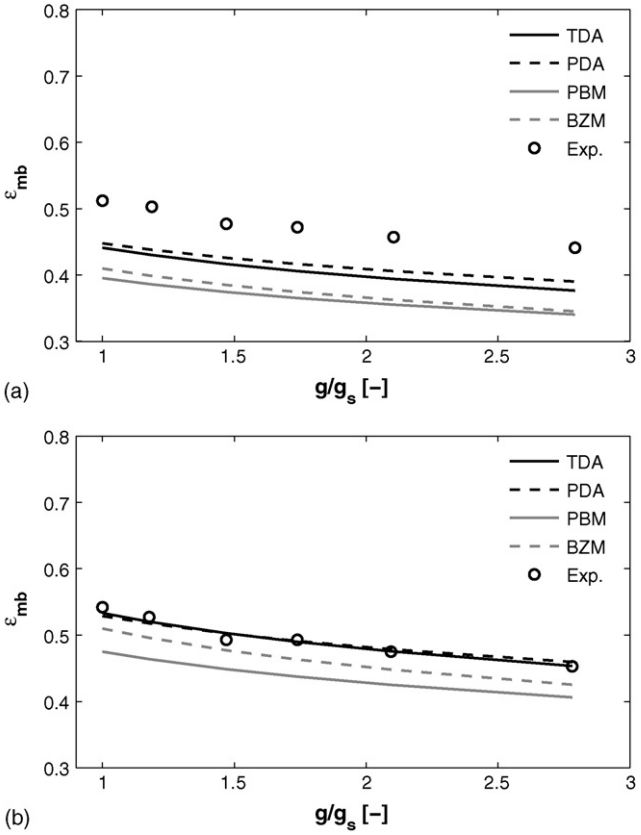


**Fig. 5.** Gravitational field strength effect on MBV of FCC catalyst particles [38]: (a) incremented gravity (hydrogen) and (b) incremented gravity (nitrogen).

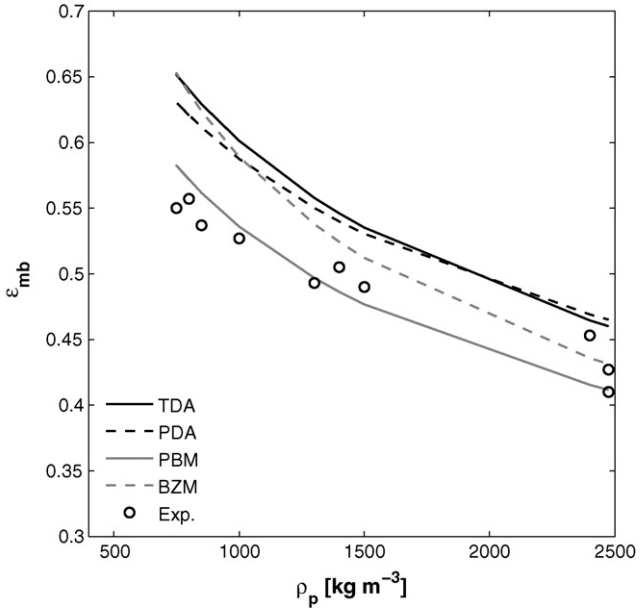


**Fig. 6.** Experimental data reviewed by Gibilaro [16] about particle density effect on MBV of different powders (60 μm) fluidized by ambient air and model predictions.

systematic underestimation (less than 5% and 10%, respectively). It is important to point out the evidence of a systematic disagreement exhibited by all models for the cases of experiments conducted with hydrogen.

### 4.4. Particle density effect

Fig. 6 shows the effect of particle density on the MBV value. Data are extrapolated from several literature works and reviewed by Gibilaro et al. [17]. They refer to cases of fluidization of various particles having the same diameter with ambient air. As expected, MBV value decreases with particle density. The PBM prediction shows the best matching for all the systems analyzed. Conversely, BZM shows acceptable agreement only at lower MBV values. This is probably due to the sensitivity of the stability criterion. TDA and PDA show an overestimate over the entire density range (less than 11% for PDA), but a qualitatively correct trend prediction is found.

### 4.5. Particle diameter effect

Fig. 7 reports experimental data to assess the particle diameter effect [4,6,50]. In particular, Fig. 7(c) shows a system exhibiting always particulate fluidization at lower diameters and transition to bubbling fluidization at higher diameters. PBM and BZM are not able to predict such transition, while TDA and PDA show the correct trend, with fairest agreement for TDA (error less than 10%). Also for the case of the experimental data reported in Fig. 7(b) and (c) similar considerations apply. PBM gives a good agreement only for systems with low MBV value. The BZM predictions also follow a correct trend at low MBV values. Both PBM and BZM show in fact significant levels of overestimation for systems with high MBV due to the numerical sensitivity of the linear stability criterion. Conversely, TDA predictions provide better agreement with minimum underestimate for large diameters (less than 6%) and slightly higher overestimates for small diameters.

An effort has been made to discuss the effect of particle forces. When interparticle bounding forces are higher than particle weights, a cohesive behaviour of powders will result, or a homogeneous expansion of particle aggregates [45]. For this last case, predictions of MBV result always in homogeneous fluidization.

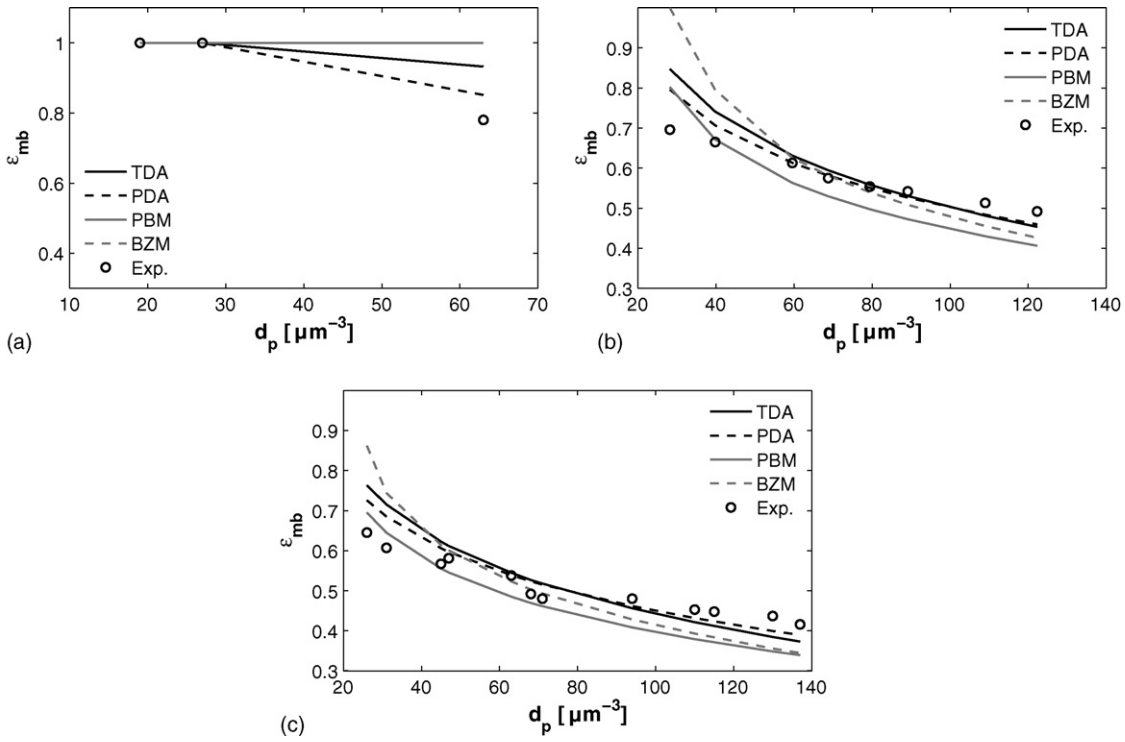


**Fig. 7.** Particle diameter effect on MBV [4,6,50]: (a) MBV of carbon powder fluidized by argon at 67 bar; (b) MBV of alumina fluidized by air; (c) MBV of FCC catalyst fluidized by air.

However, when the average size and density of aggregates [45] is taken into account, excellent agreement with experimental data is obtained, as it can be seen in Fig. 8. Notably TDA predictions give the best agreement with experiments, while PDA predictions slightly underestimate the MBV. PBM predicts the transition to bubbling only for the largest particles, while BZM predicts always homogeneous fluidization for the smallest particle sizes, and a sudden decrease of MBV at larger particle diameters. Such results underline the crucial importance of the modelling of interparticle forces for small (or light) particles (*i.e.* for the prediction of aggregates properties), and highlights that the behaviour of the resulting aggregates is fully described by the governing equations of fluid motion.

### 4.6. Overall predictivity

On overall, the predictions obtained by the stability criteria derived from the presented model in its mono-dimensional formulation show good agreement of predictions with relevant experimental data. As it can be seen in Fig. 9, TDA and PDA give rise to the lowest data dispersion, especially at higher MBV values (where PBM and BZM are not able to predict the transition from homogeneous to bubbling fluidization). In particular, PDA shows the minimum data dispersion between all models.

Each model presents its own distribution of prediction residuals (*i.e.* difference between model predictions and experimental data). In particular, the mean value of percentage residual and relevant standard deviation (STD) are used to characterize the residual

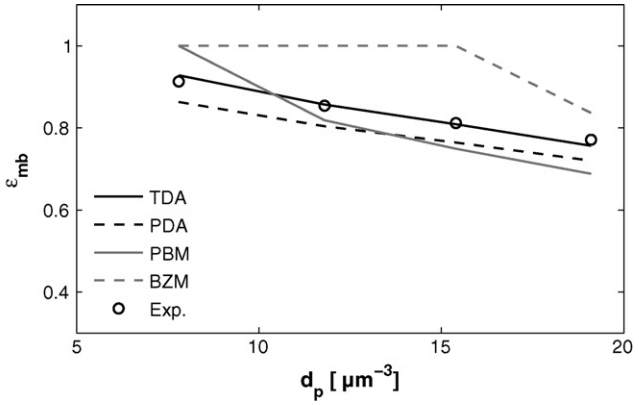


**Fig. 8.** Experimental data by Valverde et al. [45] about particle diameter effect on MBV of different additivated toners fluidized by nitrogen and model predictions by using aggregates average size and density measured by the same authors.

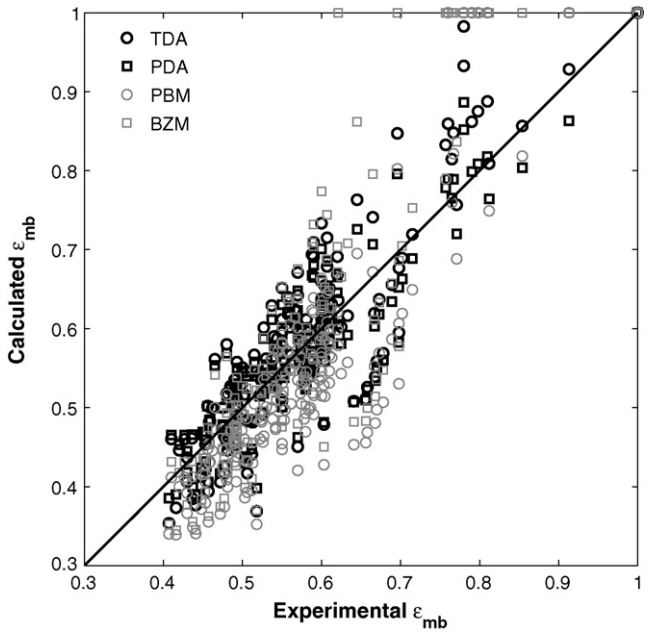


**Fig. 9.** Comparison between MBV experimental values and model predictions.

**Table 2**
Fitting parameters values.

| Approach | % Mean | % STD |
|---|---|---|
| PDA | 0.07 | 8.48 |
| TDA | 1.63 | 9.93 |
| PBM | 1.30 | 14.08 |
| BZM | −6.91 | 11.17 |

distribution, as reported in Table 2. It is worth noting that mean residuals are in the range of ±2% with the exception of BZM, and relevant standard deviation lie in the range ±15%. TDA and PDA show the smaller values of both mean value and standard deviations, with best results obtained by PDA.

For the sake of comparison, as an alternative to the Richardson–Zaki equation for the drag force, overall predictions obtained by means of Eqs. (19) and (20) are shown in Fig. 10. Unexpectedly, the such predictions lead to worse agreements, especially for systems exhibiting high MBV. This is due to the fact that the elastic force depends on the derivative of the drag force with respect to voidage, rather than the drag force value itself.

It is worth noting that with reference to the literature data here analyzed, both TDA and PDA correctly describe the behaviour of particulate systems with MBV equal to one (*i.e.* those systems not showing a transition from homogeneous to bubbling fluidization). Conversely, PBM and BZM results in predicting values of MBV equal to one in 7 and 14 systems here examined, respectively, for systems having MBV less than unity.

Using the stability criteria derived from TDA and PDA, a predicted Geldart chart for fluidization with ambient air can be obtained, as shown in Fig. 11. The separation line between group-A and group-B powders is obtained by finding the density-diameter couples with MBV value equal to 0.40 (*i.e.* for which MBV is equal to the maximum packing voidage value), while the separation line between group-B and group-D powders is obtained by finding the density-diameter couples for which MBV value is equal 0.1, on the base of fluidization quality considerations [16]. It is evident from Fig. 11 the sound agreement between model predictions and the well-known Geldart chart.

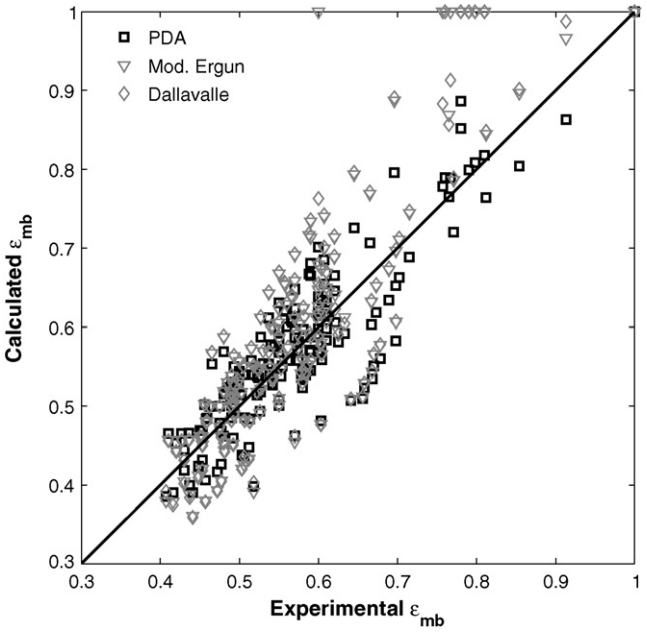


**Fig. 10.** Comparison between MBV experimental values and PDA predictions when using different drag force expressions.

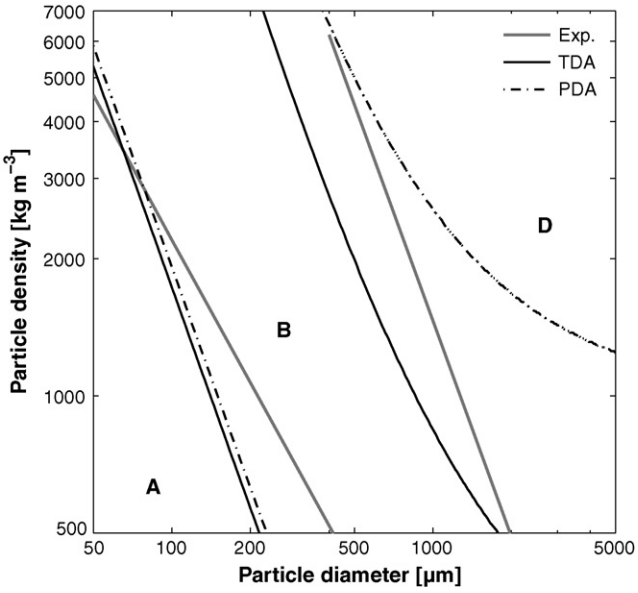


**Fig. 11.** Experimental Geldart chart and predicted chart by TDA and PDA.

## 5. Comparison of alternative stability functions

All functional dependencies of the stability function for TDA, PDA, PBM and BZM were analyzed. In general the stability function for each model takes the form reported in Eq. (32). Each model, in particular, is characterized by its own definition of the dynamic wave velocity, leading to different functional dependencies of the stability function. In the case of PBM and BZM, a characteristic asymmetrical U-shaped stability function is obtained, as it can be easily observed in Fig. 12, where all the stability function for a particular test case have been reported as a function of voidage $\epsilon$. These curves exhibit a descending section at low voidage, a plateau section and a suddenly increasing asymptote at voidage values approaching to one. This is a marked difference with respect to the monotone decreasing dependence of the stability function for both TDA and PDA. Different systems show different values

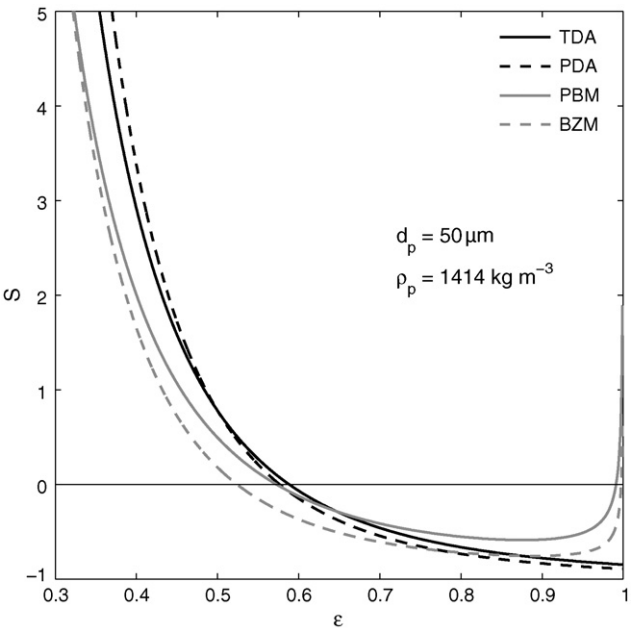


**Fig. 12.** Typical stability function plot for Geldart-A powder.

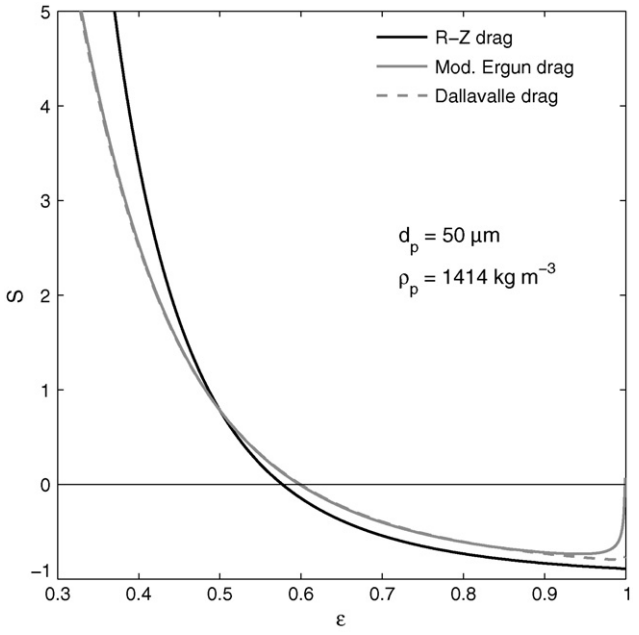


**Fig. 13.** Influence of drag force correlation on TDA stability function plot for Geldart-A powder.

of the stability function, but the shape remains substantially the same.

The lower value of the two roots of the stability function is the $\epsilon$ value corresponding to incipient bubbling conditions. Gibilaro [16] found that the higher value of the two roots corresponds to the bubble phase voidage value. On this ground, the newly formulated models are not able to predict this second root, because of the monotonic behaviour of the relevant stability functions.

Nevertheless, the U-shaped stability functions of PBM and BZM lead to the impossibility of predicting MBV values lying on the right-hand side of the minimum value of the stability function itself. This in practice cancels out the possibility of predicting MBV values higher than 0.80 for PBM and 0.85 for the BZM.

It is worth noting that different expressions of near-equilibrium drag force results in different dependencies on voidage, as reported in Fig. 13. In particular, U-shaped curves result for Dallavalle and modified Ergun drag formulation. This occurrence leads to the existence of two roots, whose physical meaning was discussed above, but negatively affects the model predictivity at high MBV values, as seen in Fig. 10. It should be therefore emphasized the importance of selecting the Richardson–Zaki drag expression [16], which best describes the voidage dependence of drag force for homogeneously fluidized beds.

On overall, TDA and PDA stability functions show an increased robustness for prediction of MBV with respect to PBM and BZM, thanks to the monotonic dependence on voidage of the stability function. This feature makes possible to predict MBV values over the entire range. The information from the second root of the PBM stability function can not be obtained by TDA and PDA, however, both approaches have the noticeable advantage of an accurate and robust fully predictivity.

## 6. Conclusions

The proposed linear stability criteria have been derived starting from the formulation of the PBM as revisited by [2], with the aim to purposely introduce an averaging length on the basis of a theoretical analysis at incipient bubbling fluidization.

In particular, the stability criteria were obtained by introducing an alternative elastic term and a new voidage dependency on the local elastic properties in both the fluid and particle phase momentum equations. The balance equations thus obtained were suitably coupled and linearized to derive the stability criteria.

Validation of the proposed model was carried out by means of a simple mono-dimensional linear stability analysis. From such analysis two different criteria to predict the onset of bubbling resulted. Predictions so far obtained on the base of the proposed stability criteria were finally compared with literature data available. On overall the agreement was found good particularly for the case of systems characterized by high values of MBV, where the previously developed models (*i.e.* PBM and BZM) were not able to make reliable predictions.

This is mainly due to the characteristic monotonic dependence on voidage of the newly developed stability functions, which are markedly different from those of PBM and BZM.

## References

[1] T. Anderson, R. Jackson, A fluid mechanical description of fluidized beds. equation of motion, Ind. Eng. Chem. Fundam. 6 (1967) 527–539.
[2] S. Brandani, K. Zhang, A new model for the prediction of the behaviour of fluidized beds, Powder Technol. 163 (2006) 80–87.
[3] C. Crowe, M. Sommerfeld, Y. Tsujii, Multiphase Flow with Droplets and Particles, CRC Press, 1998.
[4] M. Crowther, J. Whitehead, Fluidisation, Cambridge University Press, Cambridge, UK, 1978.
[5] J. Dallavalle (Ed.), Micrometrics. The Technology of Fine Particles, 2nd ed., Pitman, London, 1948.
[6] J. De Jong, J. Nomden, Homogeneous gas–solid fluidization, Powder Technol. 9 (1974) 91.
[7] R. Di Felice, The voidage function for fluid particle interaction systems, Int. J. Multiphase Flow 20 (1994) 153–159.
[8] D. Drew, Mathematical modelling of two phase flow, Annu. Rev. Fluid Mech. 83 (1983) 261–291.
[9] H. Enwald, E. Peirano, A. Almstedt, Eulerian two phase flow theory applied to fluidization, Int. J. Multiphase Flow 22 (Suppl. 1) (1996) 21–66.
[10] S. Ergun, Fluid flow through packed columns, Chem. Eng. Progress 48 (2) (1952) 89.
[11] P. Foscolo, L. Gibilaro, A fully predictive criterion for the transition between particulate and aggregate fluidization, Chem. Eng. Sci. 39 (1984) 1667.
[12] P. Foscolo, L. Gibilaro, Fluid dynamic stability of fluidized suspensions: the particle bed model, Chem. Eng. Sci. 42 (1987) 1489.
[13] P. Foscolo, L. Gibilaro, S. Rapagná, Infinitesimal and finite voidage perturbations in the compressible particle phase description of a fluidized bed, in: J.C. Chem (Ed.) Developments in fluidization and fluid particle systems. Vol. 91 (308) of AIChE Symposium Series, 1995, p. 44.
[14] P. Foscolo, L. Gibilaro, S. Waldram, A unified model for particulate expansion of fluidised beds and flow in fixed porous media, Chem. Eng. Sci. 38 (1983) 1251.
[15] J. Garside, M. Al-Bidouni, Velocity voidage relationship for fluidization and sedimentation, I&EC Proc. Des. Dev. 16 (1977) 206–214.
[16] L. Gibilaro, Fluidization Dynamics, Butterworth-Einemann, Oxford, UK, 2001.
[17] L. Gibilaro, R. Di Felice, P. Foscolo, On the minimum bubbling voidage and the geldart classification for fluidised beds, Powder Technol. 56 (1988) 21–29.
[18] L. Gibilaro, R. Di Felice, P. Foscolo, Added mass effect in fluidized beds: application of the Geurst Wallis analysis of inertial coupling in two phase flow, Chem. Eng. Sci. 45 (1998) 256–259.
[19] L. Gibilaro, R. Di Felice, S. Waldram, P. Foscolo, Generalized friction factor and drag coefficient correlations for fluid particle interaction, Chem. Eng. Sci. 40 (1985) 1817.
[20] D. Gidaspow, Multiphase Flow and Fluidization, Academic Press, San Diego, 1994.
[21] R. Girimonte, B. Formisani, The minimum bubbling velocity of fluidized beds operating at high temperature, Powder Technol. 189 (2009) 74–81.
[22] M. Ishii, Thermo-fluid dynamic theory of multiphase flow, Eyrolles, Paris, France, 1975.
[23] R. Jackson, The mechanics of fluidized beds: part i: the stability of the state of uniform fluidization, Trans. Inst. Chem. Eng. 41 (1963) 13–21.
[24] R. Jackson, Locally averaged equations of motion for a mixture of identical spherical particles and a Newtonian fluid, Chem. Eng. Sci. 52 (1997) 2457–2469.
[25] R. Jackson, Erratum, Chem. Eng. Sci. 53 (1998) 1955.
[26] R. Jackson, The Dynamic of Fluidised Particles, Cambridge University Press, New York, USA, 2001.
[27] K. Jacob, A. Weimer, High pressure particulate expansion and minimum bubbling of fine carbon powder, AIChE J. 33 (1987) 567.
[28] P. Lettieri, S. Brandani, J. Yates, D. Newton, A generalization of the Foscolo and Gibilaro particle-bed model to predict the fluid bed stability of some fresh fcc catalysts at elevated temperatures, Chem. Eng. Sci. 56 (2001) 5401–5412.

[29] P. Lettieri, R. Di Felice, P. Pacciani, P. Owoyemi, CFD modelling of liquid fluidized beds in slugging mode, Powder Technol. 167 (2006) 94–103.
[30] J. Li, J. Kuipers, Gas particle interactions in dense gas fluidised beds, Chem. Eng. Sci. 58 (2003) 711–718.
[31] L. Mazzei, P. Lettieri, A drag force closure for uniformly dispersed fluidized suspensions, Chem. Eng. Sci. 62 (2007) 6129–6142.
[32] L. Mazzei, P. Lettieri, T. Elson, D. Colman, A revised mono-dimensional particle bed model for fluidized beds, Chem. Eng. Sci. 61 (2006) 1958–1972.
[33] N. Menon, D. Durian, Particle motions in a gas-fluidized bed of sand, Phys. Rev. Lett. 79 (1997) 3407–3410.
[34] O. Owoyemi, P. Lettieri, R. Plac, Experimental validation of Eulerian–Eulerian simulations of rutile industrial powders, Ind. Eng. Chem. Res. 44 (2005) 9996–10004.
[35] S. Rapagná, P. Foscolo, L. Gibilaro, The influence of temperature on the quality of gas fluidization, Int. J. Multiphase Flow 20 (2) (1994) 305–313.
[36] J. Richardson, W. Zaki, Sedimentation and fluidization: part i, Trans. Inst. Chem. Eng. 32 (1954) 35.
[37] K. Rietema, E. Cottaar, H. Piepers, The effects of interparticle forces on the stability of gas-fluidized beds. ii. Theoretical derivation of bed elasticity on the basis of van der Waals forces between powder particles, Chem. Eng. Sci. 48 (9) (1993) 1687–1697.
[38] K. Rietema, S. Mutsers, The effect of gravity upon the stability of a homogeneously fluidized bed, investigated in a centrifugal field, Fluidization, Cambridge University Press, 1978.
[39] K. Rietema, H. Piepers, The effects of interparticle forces on the stability of gas-fluidized beds. ii. Theoretical derivation of bed elasticity on the basis of van der waals forces between powder particles, Chem. Eng. Sci. 45 (1990) 1627.
[40] P. Rowe, Drag forces in a hydraulic model of a fluidised bed, part ii, Trans. Inst. Chem. Eng. 39 (1961) 175.
[41] P. Rowe, Drag forces in a hydraulic model of a fluidised bed. Part ii. In: AIChE Annual Meeting. No. 58 in f, Miami Beach, 1986.
[42] M. Syamlal, W. Rogers, T. O'Brien, Mfix documentation theory guide, Technical note DOE/METC-94/1004, U.S. Department of Energy, Office of Fossil Energy, 1993.
[43] S. Tsinontides, R. Jackson, The mechanics of gas fluidized beds with an interval of stable fluidization, J. Fluid Mech. 255 (1993) 237–274.
[44] J. Valverde, A. Castellanos, Types of gas fluidization of cohesive granular materials, Phys. Rev. E 75 (2007) 031306.
[45] J. Valverde, A. Castellanos, P. Mills, M. Quintanilla, Effects of particle size and interparticle force on the fluidization behaviour of gas fluidized beds, Phys. Rev. E 67 (2003) 051305.
[46] J. Valverde, M. Quintanilla, A. Castellanos, P. Mills, Experimental study on the dynamics of gas fluidized beds, Phys. Rev. E 67 (2003) 016303.
[47] C. Vogt, R. Schreiber, G. Brunner, J. Werther, Fluid dynamics of the supercrititical fluidized beds, Powder Technol. 158 (2005) 102–114.
[48] G. Wallis, One Dimensional two-phase flow, McGraw Hill, 1969.
[49] C. Wen, Y. Yu, Mechanics of fluidization, Chem. Eng. Progress Symp. Series 62 (1966) 100.
[50] H. Xie, D. Geldart, Fluidization of fcc powders in the bubble free regime: effect of types of gases and temperature, Powder Technol. 82 (1995) 269–277.